J. Fluid Mech. (2003), *vol.* 476, *pp.* 267–292.
DOI: 10.1017/S0022112002002963 Printed in the United Kingdom

Detonation ignition from a temperature gradient for a two-step chain-branching kinetics model

By GARY J. SHARPE[1] AND MARK SHORT[2]

[1]School of Mathematics and Statistics, University of Birmingham, Edgbaston, Birmingham, B15 2TT, UK

[2]Department of Theoretical and Applied Mechanics, University of Illinois, Urbana, IL 61801, USA

(Received 20 February 2002 and in revised form 5 September 2002)

The evolution from a linear temperature gradient to a detonation is investigated for combustible materials whose chemistry is governed by chain-branching kinetics, using a combination of high-activation-temperature asymptotics and numerical simulations. A two-step chemical model is used, which captures the main properties of detonations in chain-branching fuels. The first step is a thermally neutral induction time, representing chain initiation and branching, which has a temperature-sensitive Arrhenius form of the reaction rate. At the end of the induction time is a transition point where the fuel is instantaneously converted into chain-radicals. The second step is the main exothermic reaction, representing chain termination, assumed to be temperature insensitive. Emphasis is on comparing and contrasting the results with previous studies that used simple one-step kinetics. It is shown that the largest temperature gradient for which a detonation can be successfully ignited depends on the heat release rate of the main reaction. The slower the heat release compared to the initial induction time, the shallower the gradient has to be for successful ignition. For example, when the rate of heat release is moderate or slow on the initial induction time scale, it was found that the path of the transition point marking the end of the induction stage should move supersonically, in which case its speed is determined only by the initial temperature gradient. For steeper gradients such that the transition point propagates subsonically from the outset, the rate of heat release must be very high for a detonation to be ignited. Detonation ignition for the two-step case apparently does not involve the formation of secondary shocks, unlike some cases when one-step kinetics is used.

1. Introduction

Detonation waves are powerful and rapid (supersonic) combustion waves. The power of detonations may be harnessed for engineering applications, for example in pulse detonation engines, whereas unplanned detonations represent an extreme explosion hazard. In either case, understanding how a detonation can arise from some quiescent initial conditions is crucial. There are two main ways a detonation may be ignited: either by direct ignition from a high-energy source producing a blast wave which, as it decays, transitions to a detonation, or by the creation of a small non-uniformity (in the temperature, for example) in the fuel (e.g. by slowly heating the fuel, the passage of a shock wave, the creation of a hot-spot by an accelerating

turbulent flame in a deflagration-to-detonation process or the injection of a turbulent jet into the fuel). We will be concerned with the case where the ignition process produces a temperature gradient in a region of the explosive.

A model which has been widely studied is simply that of an initial linear temperature gradient in the fuel. Most of the previous work has considered a simple chemical model in which the reaction proceeds via a single exothermic reaction, fuel → product, with Arrhenius kinetics (Jackson, Kapila & Stewart 1989; Makhviladze & Rogatykh 1991; He & Clavin 1992; Khokhlov, Oran & Wheeler 1997; Kapila *et al.* 2001). See Kapila *et al.* (2002, henceforth referred to as KSQH) for a recent review and a very detailed numerical study of the problem. The main result is that for a detonation to be ignited the temperature gradient must be sufficiently shallow to create a balance between the acoustic and reaction times at some point in the evolution. For such temperature gradients one or two shocks may be formed in the evolution process. For high gradients the balance is between diffusive and reactive times and the result is a subsonic combustion wave (flame).

Another major outcome from one-step kinetics studies is the development of diagnostic tools for interpreting the output of numerical simulations, which involve plotting snapshots of the flow profiles in the pressure–specific volume (p, V) and pressure–concentration phase planes. Clarke and co-workers (Clarke *et al.* 1990; Singh & Clarke 1992; Clarke & Nikiforakis 1999) have shown that straight lines with negative slope in the (p, V)-plane represent a quasi-steady wave phenomenon (waves whose speed and structure evolve on a much slower time scale than the time it takes a particle to transit through the wave), with the slope of the line being proportional to the (square of the) mass flux through the wave. This has been very successfully exploited in a number of ignition studies (Clarke *et al.* 1990; Singh & Clarke 1992; Dold *et al.* 1995; Nikiforakis & Clarke 1996; KSQH) which show that the reaction zone evolution may involve decelerating quasi-steady weak detonations (shockless reaction waves through which pressure and density increase and the flow is everywhere supersonic in the wave's rest frame), quasi-steady fast flames (diffusionless subsonic combustion waves through which pressure and density decrease), as well as shocks and completely unsteady reactive regions, their interactions and transitions from one to another. The pressure–concentration diagrams clearly reveal the location of events inside the reaction zone, such as the birthplace of shocks. In this paper we exploit these diagnostic tools throughout to classify the ignition evolution.

Detonations in fuels such as hydrogen–oxygen and hydrocarbon–oxygen have well-defined induction zones followed by exothermic main reaction zones (Fickett, Jacobson & Schott 1972). The ratio of the length scale of the induction zone to that of the main reaction zone in these detonations depends on the initial conditions. For example in hydrogen–oxygen at low pressures the main reaction zone is much longer than the induction zone, but at higher pressures the two length scales become comparable (Fickett *et al.* 1972). The chemistry in these fuels is governed by chain-branching kinetics, with the induction zone corresponding to slightly endothermic but temperature-sensitive chain initiation and branching reactions and the exothermic main reaction zone to that of chain recombination or termination reactions. For many condensed-phase (solid and liquid) explosives the reactions proceed in a similar manner, with an initial induction stage in which molecular bonds are broken down, followed by a state-insensitive exothermic recombination stage (Dremin 1999). In powerful condensed-phase explosives the induction zone may be extremely short compared to the main reaction zone length, perhaps due to the creation of active particles in non-equilibrium processes inside the leading shock wave (Dremin 1999).

A single Arrhenius reaction model cannot reproduce the features of detonations governed by chain-branching kinetics described above because, in order to have a well-defined induction zone for one-step chemistry, the activation temperature must be high, but then the main reaction layer becomes exponentially thin. Indeed, it has been shown that for shock ignition of detonations, qualitatively different results may be obtained using chain-branching chemistry models than found for one-step chemistry (Dold & Kapila 1991; Sharpe 2002). It is therefore important to investigate and understand the qualitative differences in the ignition process from a temperature gradient between chain-branching kinetics and the predictions from one-step models.

In order to investigate the ignition of detonation in fuels with chain-branching kinetics a model is used in this paper which is based on a widely used two-step chemistry description, which mimics the essential features described above. The model consists of a temperature-sensitive induction stage, at the end of which the fuel is converted instantaneously into chain-radicals, followed by an exothermic main reaction (or chain recombination) stage. Such two-step induction time–heat release models are used for numerical simulations of unstable detonations in hydrogen–oxygen mixtures or liquid nitromethane (e.g. Taki & Fujiwara 1978; Guirguis, Oran & Kailasanath 1986). For numerical simulations of shock-induced ignition, such models, when fitted to data from homogeneous explosion calculations, can give very good agreement with full reaction kinetics of hydrogen–oxygen–argon mixtures (Clifford *et al.* 1998). Hence, while this model is simple, it does retain the essential ingredients of chain-branching kinetics, and importantly it preserves the main qualitative difference between chain-branching and one-step kinetic models, i.e. that the temperature-sensitive initiation reactions and the main exothermic reactions are decoupled into separate stages (Fickett *et al.* 1972), the ratio of the length or time scales of which can be prescribed. In this paper the induction stage is assumed to be thermally neutral, reflecting the fact that chain initiation and chain branching are usually only weakly endothermic (Short & Quirk 1997), and since chain-recombination reactions tend to be temperature insensitive (Short & Quirk 1997), the exothermic reaction rate is assumed to be independent of temperature. The model used here has recently been employed by Short (2001) and Short & Sharpe (2002) to investigate pulsating detonations and also by Bdzil & Kapila (1992) to investigate the transformation of a shock into a detonation.

2. The model

The governing equations are the one-dimensional Reactive Euler equations, i.e. the equations of conservation of mass, momentum and energy in the reactive fluid,

$$\frac{\partial \rho}{\partial t} + u\frac{\partial \rho}{\partial x} + \rho\frac{\partial u}{\partial x} = 0, \tag{2.1}$$

$$\frac{\partial u}{\partial t} + u\frac{\partial u}{\partial x} + \frac{1}{\rho}\frac{\partial p}{\partial x} = 0, \tag{2.2}$$

$$\frac{\partial e}{\partial t} + u\frac{\partial e}{\partial x} - \frac{p}{\rho^2}\left[\frac{\partial \rho}{\partial t} + u\frac{\partial \rho}{\partial x}\right] = 0, \tag{2.3}$$

coupled to a set of chemical reaction rates. Here u is the fluid velocity, ρ the density, p the pressure and e the internal energy per unit mass.

In this paper, a two-step reaction model, representing chain-branching kinetics, is considered. The first step represents a thermally neutral chain initiation and branching

stage, or induction zone (IZ), with a temperature-sensitive Arrhenius form of the reaction rate given by

$$\frac{\partial \xi}{\partial t} + u\frac{\partial \xi}{\partial x} = k_1 \exp\left[\frac{1}{\epsilon}\left(\frac{1}{T_0} - \frac{1}{T}\right)\right], \tag{2.4}$$

where ξ is an induction time parameter, which depends on the temperature history of a particle, k_1 is a constant rate multiplier, ϵ is the inverse activation temperature, T_0 is the initial temperature and

$$T = \frac{\mu p}{R\rho} \tag{2.5}$$

is the temperature, with μ the (constant) mean molecular weight and R the universal gas constant. Initially $\xi = 0$ and the end of the induction period corresponds to $\xi = 1$, at which point the second step begins.

The second step is a temperature-insensitive but exothermic chain recombination reaction stage, or main reaction zone (MRZ). The reaction rate for this step is assumed to be of the form

$$\frac{\partial \lambda}{\partial t} + u\frac{\partial \lambda}{\partial x} = k_2(1-\lambda)^{1/2}H(\xi), \tag{2.6}$$

where λ is the chain recombination reaction progress variable (with $\lambda = 0$ at the start of the second step, while the completely burnt (all product) state corresponds to $\lambda = 1$), k_2 is the constant rate multiplier and

$$H(\xi) = \begin{cases} 0 & \text{if } \xi < 1 \\ 1 & \text{if } \xi \geqslant 1, \end{cases} \tag{2.7}$$

so that the second step is switched on for a particle only once the induction time has passed for that particle.

Here we define an 'overall' reaction progress variable, Y, by

$$Y = \begin{cases} \xi & \text{if } \xi < 1 \\ \lambda + 1 & \text{if } \xi \geqslant 1, \end{cases} \tag{2.8}$$

so that the unburnt state corresponds to $Y = 0$ and the fully burnt state to $Y = 2$, with $0 \leqslant Y < 1$ corresponding to the IZ of the reactions and $1 \leqslant Y \leqslant 2$ corresponding to the MRZ.

Equations (2.1)–(2.7) are closed by specifying an equation of state for the internal energy e. Here we use a polytropic equation of state

$$e = \frac{p}{(\gamma - 1)\rho} - Q\lambda, \tag{2.9}$$

where Q is the heat of reaction of the exothermic reaction step and γ is the (constant) ratio of specific heats. The sound speed, c, is then given by

$$c^2 = \frac{\gamma p}{\rho}. \tag{2.10}$$

We will consider uniform initial conditions apart from a linear temperature gradient, with constant pressure (and hence non-uniform density) and zero velocity with the gas initially in the completely unburnt state. The temperature is assumed to be a maximum at $x = 0$ and decreasing in the positive x-direction. As usual we will assume $x = 0$ represents a wall or a plane of symmetry (KSQH). We will assume that the temperature non-uniformity is large enough for a detonation to ignite or fail inside the non-uniformity, so we are not concerned by the conditions outside it.

The equations are non-dimensionalized by using the self-consistent scalings

$$\left.\begin{aligned} &\rho = \frac{\tilde{\rho}}{\tilde{\rho}_0}, \quad p = \frac{\tilde{p}}{\tilde{p}_0}, \quad T = \frac{p}{\rho} = \frac{\tilde{R}\tilde{\rho}_0}{\tilde{\mu}\tilde{p}_0}\tilde{T}, \quad u = \left(\frac{\tilde{\rho}_0}{\tilde{p}_0}\right)^{1/2}\tilde{u}, \quad c = \left(\frac{\tilde{\rho}_0}{\tilde{p}_0}\right)^{1/2}\tilde{c}, \\ &t = \tilde{k}_1\tilde{t}, \quad x = \left(\frac{\tilde{\rho}_0}{\tilde{p}_0}\right)^{1/2}\tilde{k}_1\tilde{x}, \quad Q = \frac{\tilde{\rho}_0}{\tilde{p}_0}\tilde{Q}, \quad k_1 = 1, \quad k_2 = k = \frac{\tilde{k}_2}{\tilde{k}_1}, \quad \epsilon = \frac{\tilde{\mu}\tilde{p}_0}{\tilde{R}\tilde{\rho}_0}\tilde{\epsilon}, \end{aligned}\right\} \tag{2.11}$$

where $\tilde{p}_0$ is the initial pressure and $\tilde{\rho}_0$ is the initial density at $x = 0$ and a tilde denotes dimensional quantities. The dimensionless initial state is given by

$$p = 1, \quad T = 1 - \epsilon a x, \quad u = 0, \quad c^2 = \gamma(1 - \epsilon a x), \quad \xi = 0, \quad \lambda = 0. \tag{2.12}$$

Note that here x and t have been scaled using the rate constant for the induction step $\tilde{k}_1$, so that these represent IZ length and time scales. However, since there are two distinct time scales in the problem corresponding to the IZ and MRZ, one could alternatively non-dimensionalize space and time using the MRZ rate constant, $\tilde{k}_2$, to give scaled variables, x_{MRZ} and t_{MRZ} say, as measured on the MRZ scales. The relation between the IZ and MRZ scaled variables are simply

$$t_{\mathrm{MRZ}} = kt, \quad x_{\mathrm{MRZ}} = kx, \tag{2.13}$$

where k is the ratio of the main reaction step rate constant to that of the induction step (i.e. the ratio of the reaction times of the two steps), and then the temperature gradient as measured on the MRZ scale, a_{MRZ}, is given by

$$a_{\mathrm{MRZ}} = \frac{a}{k}. \tag{2.14}$$

In the two-step model, there is no heat release during the induction stage (representing the fact that this stage is usually only very slightly endothermic). Hence until the induction time parameter first reaches unity (which occurs at $x = 0$ since the temperature is a maximum there), the temperature, pressure and gas velocity remain unchanged. This is markedly different from the one-step model, for which there is a small amount of heat release during the induction stage that nevertheless switches on gas dynamics due to the temperature-sensitive nature of the reaction (KSQH). Hence, for the two-step model, during this stage the induction time parameter is simply governed by

$$\frac{\partial \xi}{\partial t} = \exp\left[\frac{1}{\epsilon}\left(1 - \frac{1}{1 - \epsilon a x}\right)\right], \tag{2.15}$$

which integrates to give

$$\xi = \exp\left[\frac{1}{\epsilon}\left(1 - \frac{1}{1 - \epsilon a x}\right)\right] t, \tag{2.16}$$

Hence ξ first reaches unity at $x = 0$ at time $t = 1$. It is hence convenient to shift the timescale by defining

$$\tau = t - 1, \tag{2.17}$$

so that ignition first occurs at $\tau = 0$.

In order to determine what happens subsequent to ignition, consider first the spontaneous wave concept of Zeldovich (1980), i.e. suppose that the gasdynamics is switched off, and hence the induction time for a particle is determined only by the initial conditions for that particle. Then (2.16) remains valid for $\tau > 0$, and the transition point marking the end of the IZ and the start of the MRZ (which may

properly be termed the ignition point when the heat release is very rapid, $k \gg 1$), i.e. the point where $\xi(x,\tau) = Y(x,\tau) = 1$, would propagate along the path in (x,τ)-space given by

$$\tau = \exp\left[-\frac{1}{\epsilon}\left(1 - \frac{1}{1-\epsilon a x}\right)\right] - 1. \tag{2.18}$$

The speed of the transition point is hence given by

$$\frac{\mathrm{d}x}{\mathrm{d}\tau} = \frac{(1-\epsilon a x)^2}{a}\exp\left[\frac{1}{\epsilon}\left(1 - \frac{1}{1-\epsilon a x}\right)\right]. \tag{2.19}$$

For large activation temperature ($\epsilon \ll 1$) and $ax = O(1)$,

$$\frac{\mathrm{d}x}{\mathrm{d}\tau} \approx \frac{1}{a}\mathrm{e}^{-ax}. \tag{2.20}$$

The transition point thus decelerates as it propagates to the right, but it propagates supersonically (faster than the local sound speed) if

$$\frac{\mathrm{d}x}{\mathrm{d}\tau} > (\gamma(1-\epsilon a x))^{1/2}, \tag{2.21}$$

i.e. if

$$x < \frac{1}{a}\ln\left(\frac{1}{\gamma^{1/2}a}\right) \tag{2.22}$$

for large activation temperature. Hence if the temperature gradient is sufficiently shallow, $a < \gamma^{-1/2}$, then the transition point will initially move away from $x = 0$ supersonically, but decelerates until it becomes sonic at $x \approx \ln(1/\gamma^{1/2}a)/a$, and subsequently propagates subsonically. For steeper gradients, however, the transition point will propagate subsonically from the outset.

Of course, the heat release of the second step will disturb the initial state and switch on the gasdynamics, increasing the pressure and temperature and driving fluid motion. This disturbance will then initially propagate away from $x = 0$ at the local sound speed. For shallow gradients such that the transition point initially propagates supersonically, no disturbances (apart from shocks) from the MRZ behind the transition point can overtake it and hence it will continue to propagate along the path given by (2.18) until it slows to sonic speed (or is overtaken by a shock wave formed in the MRZ). Hence during this time the transition point follows the path of the spontaneous wave. Again, this is different to the one-step model where the small amount of heat released during the induction stage switches on the gasdynamics before ignition (thermal runaway) occurs at $x = 0$. Hence for one-step kinetics the gasdynamical state ahead of the ignition point is not the initial state. Due to the temperature-sensitive nature of the reaction this can lead to the ignition point propagating along a path quite different from that predicted by the spontaneous wave path (KSQH).

During the early stages the heat release in the MRZ increases the pressure and hence drives fluid motion forward. However, there must then be a rarefaction wave near $x = 0$ to reduce the gas velocity back to zero there. The strength of this expansion wave depends on the temperature gradient (KSQH), but at early times before the gas at $x = 0$ is fully burnt, the MRZ must span the compressive and expansive regions between the transition point and $x = 0$. Thus in the early stages the MRZ must consist of a compressive region immediately behind the transition point, followed by an expansive region back to $x = 0$. Only once the fuel at the wall is completely

burnt (which takes an $O(1/k)$ time) and the MRZ subsequently moves away from the region $x = 0$ and the associated rarefaction can the MRZ become a fully compressive region.

Once the transition point speed becomes subsonic, the disturbances from the MRZ will overtake it. For sufficiently steep temperature gradients this will occur at $\tau = 0$ since then the transition point propagates subsonically from the outset. The temperature in the IZ region ahead of the transition point will then be increased, causing a decrease in the induction time and hence accelerating the transition point, so that it will move ahead of the path given by (2.18).

What happens for a given temperature gradient depends on how fast the exothermic reaction is (i.e. how rapid the heat release is). In this paper we will investigate the behaviour for three cases: when the rate of heat release is slow (i.e. the reaction time of the second step is long) compared to the initial induction time (represented by $k = 0.25$); when the rate of heat release is comparable to the initial induction time (represented by $k = 5$) and when the heat release is rapid compared to the initial induction time (represented by $k = 100$).

In this paper we fix the heat release and ratio of specific heats to be $Q = 4$ and $\gamma = 1.2$, respectively, while for the numerical simulations the inverse activation temperature is set to be $\epsilon = 1/20$, and then vary a and k.

3. Slow heat release: high-activation-temperature asymptotics

It is instructive to first consider the case $k = \tilde{k}_2/\tilde{k}_1 \ll 1$, so that the heat release time is long compared to the initial induction period. In this case it is possible to carry out a high-activation-temperature asymptotic analysis, i.e. it is assumed that $\epsilon \ll 1$, for $\tau = O(1)$. The long heat release period is then expressed by assuming $k \sim O(\epsilon)$ ($k = \epsilon K$, say). The dependent variables are then expanded as

$$\rho = 1 + \epsilon\rho_1, \quad p = 1 + \epsilon p_1, \quad T = 1 + \epsilon T_1, \quad u = \epsilon u_1, \quad \lambda = \epsilon\lambda_1. \tag{3.1}$$

Note that at $\tau = 0$,

$$p_1 = u_1 = \lambda_1 = 0, \quad T_1 = -ax. \tag{3.2}$$

For $O(1)$ times, (2.1)–(2.3) can be written to leading order as

$$\frac{\partial\rho_1}{\partial\tau} + \frac{\partial u_1}{\partial x} = 0, \tag{3.3}$$

$$\frac{\partial u_1}{\partial\tau} + \frac{\partial p_1}{\partial x} = 0, \tag{3.4}$$

$$\frac{\partial T_1}{\partial\tau} - (\gamma - 1)\frac{\partial\rho_1}{\partial\tau} = \beta\frac{\partial\lambda_1}{\partial\tau} = \beta K H(\xi), \tag{3.5}$$

where $\beta = (\gamma - 1)Q$, and since $T = p/\rho$,

$$T_1 = p_1 - \rho_1. \tag{3.6}$$

Defining

$$\chi = \frac{x}{\gamma^{1/2}}, \quad U_1 = \gamma^{1/2}u_1 \tag{3.7}$$

(note that χ is then distance scaled using the initial sound speed at $x = 0$), (3.3)–(3.5) can be re-written in characteristic form as

$$\left(\frac{\partial}{\partial\tau} \pm \frac{\partial}{\partial\chi}\right)(p_1 \pm U_1) = \beta K H(\xi), \tag{3.8}$$

$$\frac{\partial T_1}{\partial\tau} = \frac{(\gamma-1)}{\gamma}\frac{\partial p_1}{\partial\tau} + \frac{\beta K}{\gamma}H(\xi). \tag{3.9}$$

Hence, at leading order, the positive characteristics are straight lines in the (χ,τ)-plane on which $\mathrm{d}\chi/\mathrm{d}\tau = 1$, and represent waves travelling to the right at the initial sound speed (unity in (χ,τ)-coordinates), on which

$$\frac{\mathrm{d}}{\mathrm{d}\tau}(p_1 + U_1) = \beta K H(\xi). \tag{3.10}$$

Similarly, the negative characteristics are straight lines in the (χ,τ)-plane with slope -1, representing waves travelling to the left at the leading-order sound speed, on which

$$\frac{\mathrm{d}}{\mathrm{d}\tau}(p_1 - U_1) = \beta K H(\xi). \tag{3.11}$$

The leading-order particle paths are lines of constant χ on which

$$\frac{\mathrm{d}}{\mathrm{d}\tau}\left(T_1 - \frac{(\gamma-1)}{\gamma}p_1\right) = \frac{\beta K}{\gamma}H(\xi). \tag{3.12}$$

As we shall see, for a detonation to be ignited when k is small, the temperature gradient has to be sufficiently shallow on the IZ scale, such that the transition point initially propagates supersonically. Indeed, the temperature gradient a has to be very small for detonation ignition in this case, and hence the initial speed of the transition point rather high. Therefore we will only consider the case of a supersonic transition path, which is then determined only by the initial conditions, and from (2.18), to leading order for $\epsilon \ll 1$, is given by

$$\tau = \exp(a\gamma^{1/2}\chi) - 1. \tag{3.13}$$

The IZ consists of the region of (χ,τ)-space ahead of the transition point, $\tau < \exp(a\gamma^{1/2}\chi) - 1$, and remains undisturbed since there is no heat release there, while the MRZ occupies the region $\tau > \exp(a\gamma^{1/2}\chi) - 1$. All the negative characteristics originate from the initial state at $\tau = 0$. The initial disturbance from the heat release due to ignition at $\chi = 0$ at $\tau = 0$ propagates along the positive characteristic $\tau = \chi$. This first characteristic from the disturbed region separates two different regions of the MRZ. For any point in the region of the MRZ ahead of this characteristic, $\exp(a\gamma^{1/2}\chi) - 1 < \tau < \chi$, the positive characteristic through that point originates from the initial state at $\tau = 0$. However, for any point in the region of the MRZ behind this characteristic, $\tau > \chi$, the positive characteristic originates at $\chi = 0$ at some time $\tau > 0$.

Consider first a point (χ,τ) in the region of the MRZ ahead of the positive characteristic from $(0,0)$. The negative characteristic through this point intersects the transition path given by (3.13) at the point (χ_-,τ_-) given by

$$\exp(a\gamma^{1/2}\chi_-) + \chi_- - 1 = \chi + \tau, \quad \tau_- = \exp(a\gamma^{1/2}\chi_-) - 1 \tag{3.14}$$

(note that (3.14) requires the straightforward numerical solution for χ_-). On this

negative characteristic, (3.11) can be integrated to give

$$p_1 - U_1 = \beta K(\tau - \tau_-), \tag{3.15}$$

where the matching condition with the undisturbed IZ region that $p_1 - U_1 = 0$ there has been employed on the transition path.

The positive characteristic through the point (χ, τ) intersects the transition path at (χ_+, τ_+) given by

$$\exp(a\gamma^{1/2}\chi_+) - \chi_+ - 1 = \tau - \chi, \quad \tau_+ = \exp(a\gamma^{1/2}\chi_+) - 1. \tag{3.16}$$

On this positive characteristic, (3.10) integrates to give

$$p_1 + U_1 = \beta K(\tau - \tau_+), \tag{3.17}$$

again employing the matching condition with the undisturbed IZ on the transition path.

Equations (3.15) and (3.17) give

$$p_1 = \beta K\tau - \frac{\beta K}{2}(\tau_- + \tau_+), \quad U_1 = \frac{\beta K}{2}(\tau_- - \tau_+) \quad \text{at } (\chi, \tau). \tag{3.18}$$

Alternatively, consider a point (χ, τ) behind the positive characteristic from $(0, 0)$. On the negative characteristic through this point, (3.14) and (3.15) still hold. However, the positive characteristic through this point now originates from $\chi = 0$ at time τ_0 given by

$$\tau_0 = \tau - \chi \tag{3.19}$$

and does not intersect the transition path.

At $\chi = 0$, $U_1 = 0$ due to the symmetry condition there, while the value of p_1 at $(0, \tau_0)$ needs to be determined. The negative characteristic through $(0, \tau_0)$ intersects the transition path at (χ'_-, τ'_-) given by

$$\exp(a\gamma^{1/2}\chi'_-) + \chi'_- - 1 = \tau_0 = \tau - \chi, \quad \tau'_- = \exp(a\gamma^{1/2}\chi'_-) - 1. \tag{3.20}$$

Integrating (3.11) along this negative characteristic gives

$$p_1 = \beta K(\tau_0 - \tau'_-) \quad \text{at } (0, \tau_0). \tag{3.21}$$

Now, integrating (3.10) along the positive characteristic through (χ, τ) gives

$$p_1 + U_1 = \beta K(\tau - \tau'_-), \tag{3.22}$$

after applying (3.21) at $(0, \tau_0)$. Equations (3.15) and (3.22) give

$$p_1 = \beta K\tau - \frac{\beta K}{2}(\tau_- + \tau'_-), \quad U_1 = \frac{\beta K}{2}(\tau_- - \tau'_-). \tag{3.23}$$

Once the pressure perturbation has been determined everywhere, the temperature is determined by integrating (3.12) along the particle path (line of constant χ) through any point (χ, τ). The full solution is then

$$p_1 = \begin{cases} 0, & \tau < \exp(a\gamma^{1/2}\chi) - 1 \\ \beta K\tau - \beta K(\tau_- + \tau_+)/2, & \exp(a\gamma^{1/2}\chi) - 1 < \tau < \chi \\ \beta K\tau - \beta K(\tau_- + \tau'_-)/2, & \chi < \tau, \end{cases} \tag{3.24}$$

$$U_1 = \begin{cases} 0, & \tau < \exp(a\gamma^{1/2}\chi) - 1 \\ \beta K(\tau_- - \tau_+)/2, & \exp(a\gamma^{1/2}\chi) - 1 < \tau < \chi \\ \beta K(\tau_- - \tau'_-)/2, & \chi < \tau, \end{cases} \tag{3.25}$$

$$T_1 = \begin{cases} -a\gamma^{1/2}\chi, & \tau < \exp(a\gamma^{1/2}\chi) - 1 \\ (\gamma-1)p_1/\gamma + \beta K(\tau - \tau_p)/\gamma - a\gamma^{1/2}\chi, & \exp(a\gamma^{1/2}\chi) - 1 < \tau, \end{cases} \tag{3.26}$$

$$\lambda_1 = \begin{cases} 0, & \tau < \exp(a\gamma^{1/2}\chi) - 1 \\ K(\tau - \tau_p), & \exp(a\gamma^{1/2}\chi) - 1 < \tau, \end{cases} \tag{3.27}$$

where τ_p is the intersection of the particle path through any point (χ, τ) in the MRZ with the transition path, given by

$$\tau_p = \exp(a\gamma^{1/2}\chi) - 1, \tag{3.28}$$

while τ_-, τ_+ and τ'_- are given in terms of χ and τ by (3.14), (3.16) and (3.20), respectively, all of which require straightforward numerical solution. Note that the spatial pressure, velocity and temperature gradients are discontinuous along $\chi = \tau$ (although the pressure, velocity and temperature themselves are continuous there). Such a weak discontinuity must propagate along a characteristic; in this case it propagates along the positive characteristic originating from $\chi = 0$ at $\tau = 0$.

Note however that when the temperature gradient is sufficiently shallow, we can determine an approximate solution to (3.24)–(3.27), since if $a \ll 1$, $\chi = O(1)$ for the MRZ, we can linearize (3.13) so that the transition path is approximately given by $\tau \approx a\gamma^{1/2}\chi$ (note that this requires $\tau = O(a)$, i.e. small time, but the transition point has propagated an $O(1)$ distance) and then

$$p_1 \approx \begin{cases} \beta K(\tau - a\gamma^{1/2}\chi), & a\gamma^{1/2}\chi < \tau < \chi \\ \beta K(1 - a\gamma^{1/2})\tau, & \chi < \tau, \end{cases} \tag{3.29}$$

$$U_1 \approx \begin{cases} \beta K a\gamma^{1/2}(\tau - a\gamma^{1/2}\chi), & a\gamma^{1/2}\chi < \tau < \chi \\ \beta K a\gamma^{1/2}(1 - a\gamma^{1/2})\chi, & \chi < \tau, \end{cases} \tag{3.30}$$

$$T_1 \approx \begin{cases} \beta K(\tau - a\gamma^{1/2}\chi) - a\gamma^{1/2}\chi, & a\gamma^{1/2}\chi < \tau < \chi \\ \beta K\left[(\gamma - (\gamma-1)a\gamma^{1/2})\tau - a\gamma^{1/2}\chi\right]/\gamma - a\gamma^{1/2}\chi, & \chi < \tau. \end{cases} \tag{3.31}$$

Hence at a given $O(a)$ time for $a \ll 1$, the MRZ approximately consists of a compressive region between the transition point at $\chi \approx \tau/(a\gamma^{1/2}) \gg \tau$ and the point $\chi = \tau$, in which pressure, velocity and temperature all increase linearly from the transition point back to $\chi = \tau$. This region is followed by a relatively small expansive region between $\chi = \tau$ and $\chi = 0$ in which the pressure is almost constant (independent of χ), the velocity decreases again so that it is zero at $\chi = 0$ (independent of τ) and the temperature continues to increase linearly but with a slightly lower gradient than in $\chi > \tau$. The pressure and velocity perturbations both reach maxima at $\chi = \tau$ of approximately $\beta K(1 - a\gamma^{1/2})\tau$ and $\beta K a\gamma^{1/2}(1 - a\gamma^{1/2})\tau$, respectively (note that the velocity perturbation therefore remains $O(a)$), while the temperature and λ perturbations are maximum at $\chi = 0$ where $T_1 \approx \beta K(\gamma - (\gamma-1)a\gamma^{1/2})\tau$ and $\lambda_1 \approx K\tau$. Note also that the density perturbation $p_1 - T_1$ in the region $a\gamma^{1/2}\chi < \tau < \chi$ is approximately $a\gamma^{1/2}\chi$, which is its initial value at a given χ, independent of τ. Hence in this region each particle is undergoing a constant-volume explosion.

It is worth noting that a similar small-time analysis is also possible when k is not small. For instance if $k = O(1)$, then rescaling time and space by $\tau = \epsilon\hat{\tau}$, $\chi = \epsilon\hat{\chi}$ and substituting these rescalings, together with the expansions (3.1), into (2.1)–(2.3) once again results in equations of the form (3.10)–(3.12) (with K replaced by k and τ replaced by $\hat{\tau}$, etc.), while the transition path again linearizes to $\hat{\tau} = a\gamma^{1/2}\hat{\chi}$ (even for $a = O(1)$ in this case). The results and main points are then very similar to those described above for small a and $k = O(\epsilon)$ (but note that the $O(\epsilon)$ temperature perturbation is zero in this case). If the heat release is rapid, $k = O(1/\epsilon)$, a very small-time analysis is then possible by rescaling time and space as $\tau = \epsilon^2\hat{\tau}$, $\chi = \epsilon^2\hat{\chi}$ with similar results.

4. Rapid heat release: weak detonations

In the limit $k \to \infty$, the MRZ lies within an $O(1/k)$ distance of the transition point which signals the end of the induction zone ($\xi = 1$). In this case, it can be shown that in a coordinate system fixed to the transition point, the following reaction wave should be quasi-steady and satisfy the usual Rankine–Hugoniot relations for a reaction discontinuity with heat addition (Bdzil & Kapila 1992; Dold, Kapila & Short 1991; Short 1997). Moreover, when the transition point moves supersonically such that its speed is greater than the Chapman–Jouguet speed, the following reaction wave must adopt the structure of a classical weak detonation (Fickett & Davis 1979). If, however, the transition point slows below Chapman–Jouguet speed, the weak detonation cannot survive, and a weak shock will form close to end of the MRZ. As the transition point continues to slow, the shock rapidly propagates through the reaction zone, and transitions the weak detonation to a strong detonation initially running close to the Chapman–Jouguet speed. This sequence of events has been described in detail by Bdzil & Kapila (1992) for a reaction model similar to that used here in the MRZ, (2.6).

For the initial temperature gradient problem considered above, there are a number of scenarios that could occur when $k \gg 1$. Let us denote the Chapman–Jouguet velocity at $x = 0$ by D_{CJ}, where

$$D_{CJ} = \frac{(2Q(\gamma^2 - 1) + 4\gamma)^{1/2} + (2Q(\gamma^2 - 1))^{1/2}}{2} \tag{4.1}$$

under the current scalings, with $D_{CJ} = 2.38$ when $Q = 4$ and $\gamma = 1.2$. Provided the temperature gradient is sufficiently small, the transition point will emerge from $x = 0$ supersonically ($a < \gamma^{-1/2}$). However, according to the description above, a weak detonation will emerge only if the speed of the transition point is above the Chapman–Jouguet speed, i.e. $\mathrm{d}x/\mathrm{d}\tau > D_{CJ}$ or $a < 1/D_{CJ} = 0.42$. In this case, the reaction wave will retain its weak detonation form until $x = x_{CJ}$, where x_{CJ} is given by

$$\frac{(1 - \epsilon a x_{CJ})^2}{a} \exp\left[\frac{1}{\epsilon}\left(1 - \frac{1}{1 - \epsilon a x_{CJ}}\right)\right] = D_{CJ}, \tag{4.2}$$

using (2.19), or for high activation temperature

$$x_{CJ} = \frac{1}{a} \ln\left(\frac{1}{aD_{CJ}}\right). \tag{4.3}$$

A transition to strong detonation is then predicted to occur near $x = x_{CJ}$, with a shock first forming close to the rear of the MRZ. If, on the other hand, $\gamma^{-1/2} > a > 1/D_{CJ}$,

the emerging wave from $x = 0$ will still be supersonic, but below the Chapman–Jouguet speed. Thus the local flow near the rear of the emerging wave will be subsonic and the whole of the MRZ cannot be a quasi-steady weak detonation in this case. Since the rear of the wave is subsonic, its structure can then be influenced by both expansion and compression waves and a transition to detonation is not guaranteed. The various scenarios for the regimes identified above when $k \gg 1$ are explored numerically below.

5. Numerical simulations

5.1. *Numerical method*

To perform the numerical simulations in this paper we use the hierarchical adaptive second-order Godunov code μCobra, which has been developed for industrial applications by Mantis Numerics Ltd. The code is fully described in Sharpe & Falle (2000). The code uses a hierarchical series of Cartesian grids $G^0, \ldots, G^N$, so that grid G^n has mesh spacing $h/2^n$, where h is the mesh spacing on the base grid G^0. Grids G^0 and G^1 cover the entire domain, but the higher grids only occupy regions where increased resolution is required. In most of the calculations the base grid spacing is 1000 mesh points per unit x, i.e. $h = 0.001$. The exception was Case III described in § 5.4 below with $a = 0.005$, $k = 0.25$ for which the transition point propagates a very large distance before detonation formation, $x \approx 1000$. Since this case required such a large domain, the base grid size was reduced to 31.25 mesh points per unit x, but with a larger number of refinement levels to compensate.

The number of refinement levels N was chosen to ensure that the results were grid independent and all the scales in the problem were fully resolved in each case. This was achieved by a set of convergence studies. It was found that the number of levels required depends on k (which determines the MRZ length scale) and a. In general larger values of a and k require more refinement levels. Between 2 and 6 refinement levels were needed for the cases considered below. The grid is refined to the highest level whenever $\lambda \leqslant 0.99$ provided $p > 1$ to ensure that both disturbed IZ and MRZ regions are refined on this level.

The initial conditions are given by those at $\tau = 0$ just prior to ignition at $x = 0$. The boundary condition at $x = 0$ is a reflective boundary condition so that this boundary is a solid, reflecting wall or a plane of symmetry.

For the cases where a was sufficiently small such that the transition point initially propagated supersonically, it was found that 'steps' in the numerical λ profile (and hence in the other variables) were produced due to the fact that the transition point propagated across several numerical cells during a time step. A simple cure for this was to make the Courant number sufficiently low during the early stages.

5.2. *Case I: $a = 0.5$*

We begin by considering a moderate value of the temperature gradient, as measured on the IZ scale, represented by $a = 0.5$. For this temperature gradient, the transition point initially propagates supersonically (for the spontaneous wave the transition point becomes subsonic at $x = 1.1$, $\tau = 0.75$), with an initial speed 2, so no disturbances can initially propagate from the MRZ into the IZ ahead of the transition point. Thus at early times the gasdynamical state of the IZ will remain undisturbed; only the MRZ behind the transition point (corresponding to $Y \geqslant 1$) will be disturbed from the initial state. However, in this case $a > 1/D_{CJ}$, so that the high-k analysis of § 4 predicts that the MRZ cannot consist completely of a quasi-steady weak detonation.

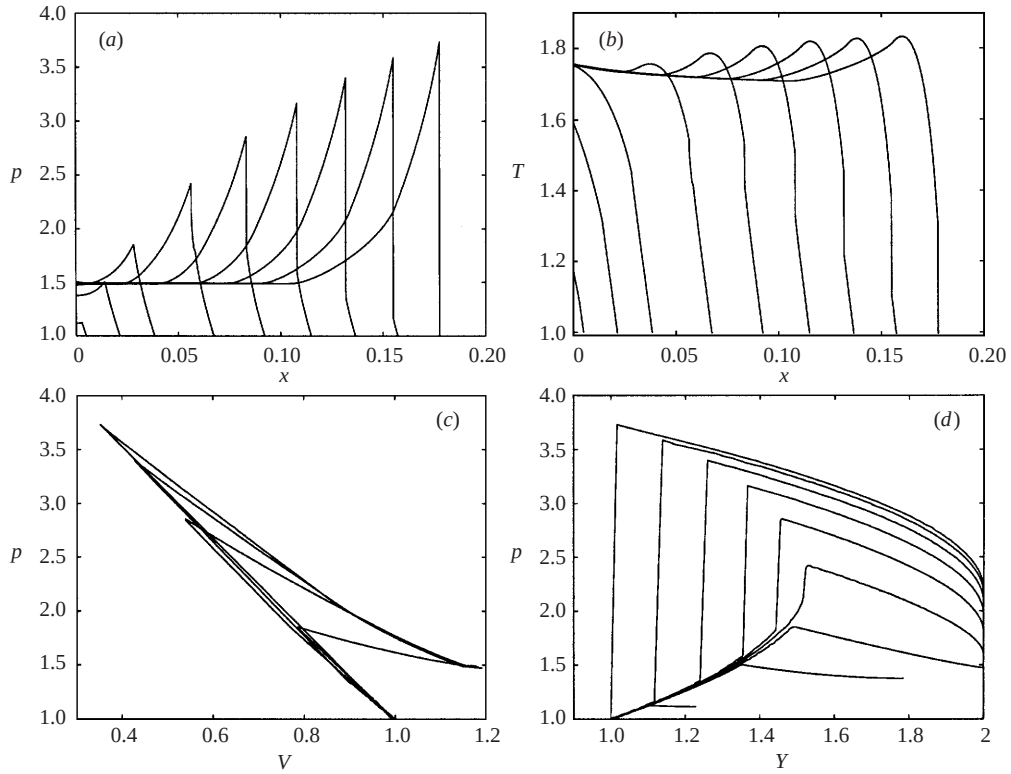

FIGURE 1. (*a*) Pressure profiles, (*b*) temperature profiles, (*c*) p, V diagrams and (*d*) p, Y diagrams for $a = 0.5$ and $k = 100.0$ at times 0.002, 0.010, 0.019, 0.034, 0.047, 0.059, 0.071, 0.08 and 0.104 (p, V diagrams only shown at times 0.019, 0.047, 0.071 and 0.104 for clarity).

Figure 1 shows the early time behaviour when the rate of heat release in the MRZ is rapid ($k = 100$, so $a_{\mathrm{MRZ}} = 0.005$). In the initial stages, before the fuel at $x = 0$ is fully burnt, the MRZ consists of a compressive region immediately behind the transition (ignition) point, followed by an expansive region back to $x = 0$ (at very early times the pressure is approximately constant in this region, in agreement with the early time analysis in § 3). These two regions are joined at a point where the pressure gradient is discontinuous. This weak discontinuity moves along the positive characteristic from $x = \tau = 0$ in the (x, τ)-plane (cf. § 3). Both the compressive and the main part of the expansive regions appear as straight lines in the p, V diagram and hence these are part of a partially reacted quasi-steady weak detonation and a quasi-steady fast flame, respectively. Evolutions which are composed of a quasi-steady weak detonation connected to a quasi-steady fast flame were first recognized by Singh & Clarke (1992) (although there is also an unsteady reactive region connecting the two quasi-steady waves in their case). The state at the pressure gradient discontinuity, which separates the weak detonation from the fast flame, initially becomes more burnt (Y increases there). Shortly after the gas at $x = 0$ becomes fully burnt, a shock can be seen to form in the interior of the MRZ, just ahead of the pressure gradient discontinuity, at about $Y = 1.5$ in the p, Y diagram. The shock quickly strengthens due to the heat release behind it, and begins to propagate through the weak detonation region of the MRZ, towards the ignition point. The slope of the fast flame increases in the p, V diagram, indicating that the mass flux through it is increasing and hence it is accelerating and

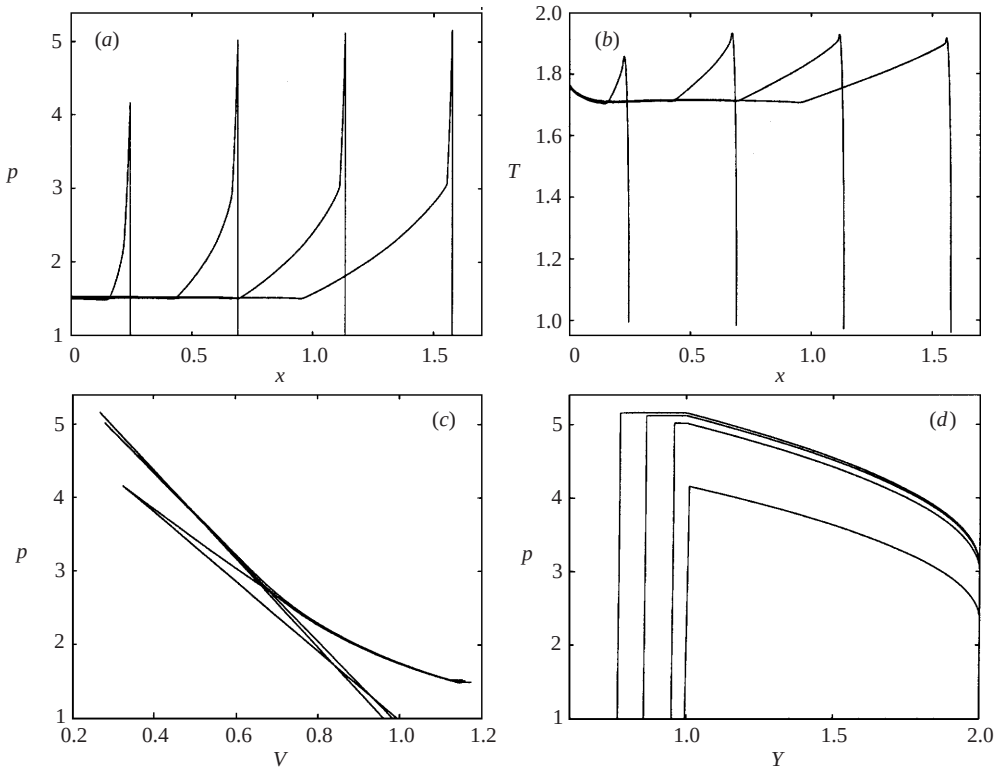

FIGURE 2. (a) Pressure profiles, (b) temperature profiles, (c) p, V diagrams and (d) p, Y diagrams for $a = 0.5$ and $k = 100.0$ at times 0.125, 0.319, 0.507 and 0.695 (p, V diagrams only shown at times 0.125, 0.319 and 0.695 for clarity).

driving the shock. At this stage then, the MRZ consists of the remaining portion of the weak detonation behind the ignition point, followed by a shock which is in turn followed immediately by the accelerating fast flame, and finally an inert expansion wave connects the end of the MRZ to $x = 0$.

The profiles shown in figure 1 bear some resemblance to the case of $a = 0.38$ studied for one-step chemistry in KSQH. However the weak detonation does not decelerate as rapidly while the shock forms much further from the end of the reaction zone in the two-step case. Indeed the shock formation shown in the p, Y diagrams is very similar to that in the pressure–progress variable diagram for $a = 1$ in KSQH for one-step kinetics.

Figure 2 shows the later time behaviour for $k = 100$. The shock overtakes the decelerating ignition point and catches up with it at $\tau = 0.10$, $x = 0.16$. Subsequently the shock propagates ahead of the ignition point, into the IZ region $Y < 1$, and hence the ignition path is no longer given by (2.18). The p, V diagrams in figure 2 show that both the shock and the fast flame continue to accelerate (the slope, and hence mass flux through both increase in the diagrams). The fast flame accelerates more quickly, however, until the shock and fast flame lie along a common line in the (p, V)-plane, i.e. they become fully coupled. At this point a quasi-steady Chapman–Jougnet (CJ) detonation is born. As the shock wave propagates into lower temperatures, the induction time, ξ, at the shock position decreases exponentially (if the shock is located at position x at time t, the induction time there is given by (2.16)). The shock raises the temperature and hence shortens the remaining induction time considerably. As

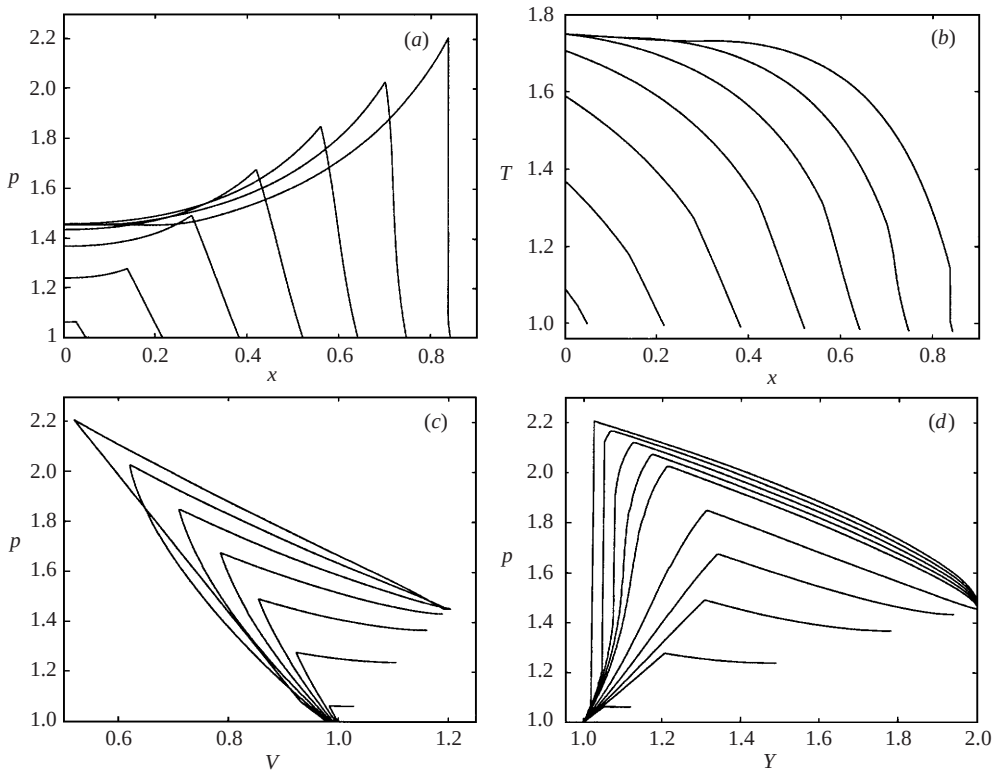

FIGURE 3. (*a*) Pressure profiles, (*b*) temperature profiles, (*c*) p, V diagrams and (*d*) p, Y diagrams for $a = 0.5$ and $k = 5.0$ at times 0.025, 0.115, 0.213, 0.303, 0.386, 0.464 and 0.538 (p, Y diagrams shown at additional times 0.483, 0.501 and 0.520 to clarify shock formation).

it propagates through decreasing values of ξ, the length of the IZ behind the shock continually increases. Note from the p, Y diagrams that the IZ of the detonation occurs at constant pressure (and temperature), attesting to the quasi-steady nature of the detonation. The pressure and temperature profiles are again very similar to the cases $a = 0.38$ and $a = 1$ described in KSQH for one-step kinetics.

Figure 3 shows the early time behaviour when the MRZ time-scale is longer and more comparable to the initial induction time ($k = 5$, so $a_{\mathrm{MRZ}} = 0.1$). At very early times the situation is very similar to that described above for $k = 100$, with a compressive region of the MRZ followed by an expansive region, and a sharp demarcation between them at a discontinuity in the pressure gradient propagating along the characteristic originating from $\tau = \chi = 0$. However, as the reaction proceeds in this case, although the expansive region for the most part lies along a straight line in the (p, V)-plane and hence represents a quasi-steady fast flame, the compressive region is unsteady (this region is curved in the p, V diagram), and so cannot be identified as a quasi-steady weak detonation process in this case. Again, the maximum pressure point first moves back to a more burnt state in the p, Y diagram, before moving forward towards the transition point so that more and more of the MRZ becomes located in the fast flame. The transition point has travelled much further before the state at $x = 0$ becomes fully burnt than for $k = 100$, due to the much slower time scale of the MRZ. The fast flame accelerates while the compressive region steepens, and shortly after the gas becomes completely burnt at $x = 0$ a shock forms in

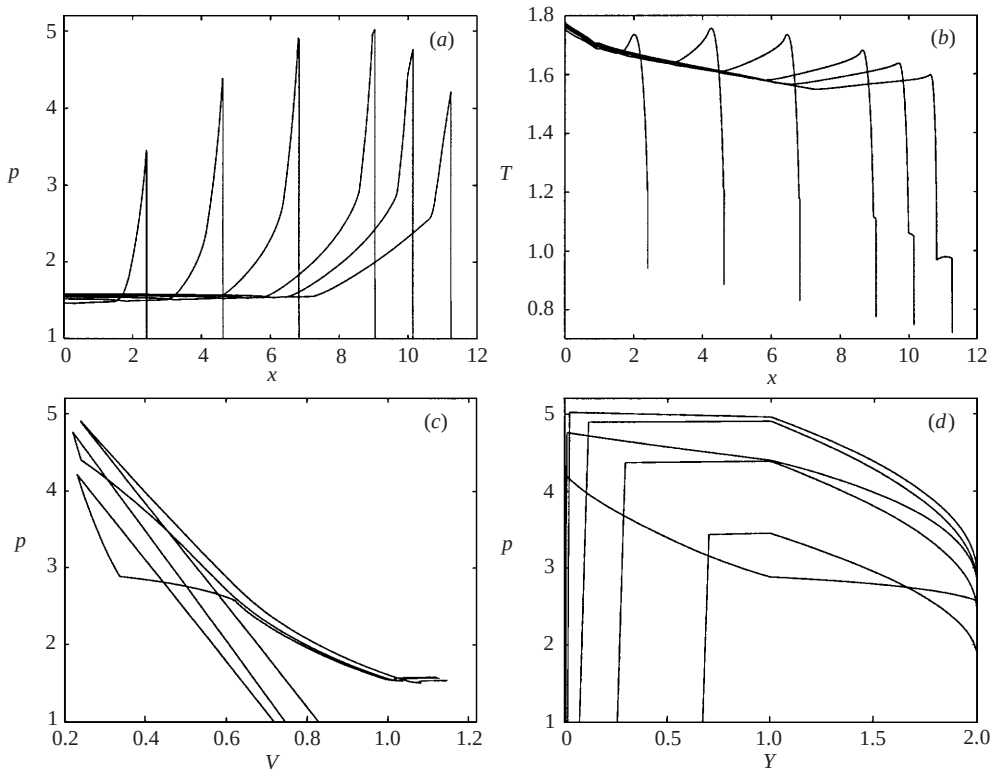

FIGURE 4. (*a*) Pressure profiles, (*b*) temperature profiles, (*c*) p, V diagrams and (*d*) p, Y diagrams for $a = 0.5$ and $k = 5.0$ at times 1.43, 2.53, 3.57, 4.62, 5.16 and 5.73 (p, V diagrams only shown at times 3.57, 5.16 and 5.73 for clarity).

the compressive part of the MRZ, but now at about $Y = 1.1$, i.e. much nearer the transition point, towards the front of the MRZ. Again, this shock then very quickly propagates through the remainder of the compressive region and then overtakes the transition point.

The profiles shown in figure 3, with an unsteady compressive region that is sharply demarcated from the quasi-steady expansive fast flame region by a discontinuity in the pressure gradient and with the shock forming near the start of the reaction zone, are not like any case for one-step kinetics studied by KSQH. They are perhaps most reminiscent of the case $a = 2$ of KSQH, but in their case the transition from the compressive to expansive region is smooth and highly curved at the peak pressure in their pressure profiles and p, V and p, Y diagrams, representing a unsteady reactive region.

Figure 4 shows the later time behaviour for $k = 5$, after the shock begins to propagate ahead of the transition point. As for $k = 100$, once the shock is formed, it and the fast flame behind it begin to accelerate and couple. During this stage the part of the IZ behind the shock is slightly compressive as can be seen in the p, Y diagrams. However, even though the shock is strengthening as it propagates into the lower temperatures ahead of it, it does not do so quickly enough to prevent the post-shock temperature from decreasing and before the shock and fast flame fully couple, the IZ behind the shock becomes expansive, the shock and reaction zone subsequently begin to rapidly decouple and the transition point falls further

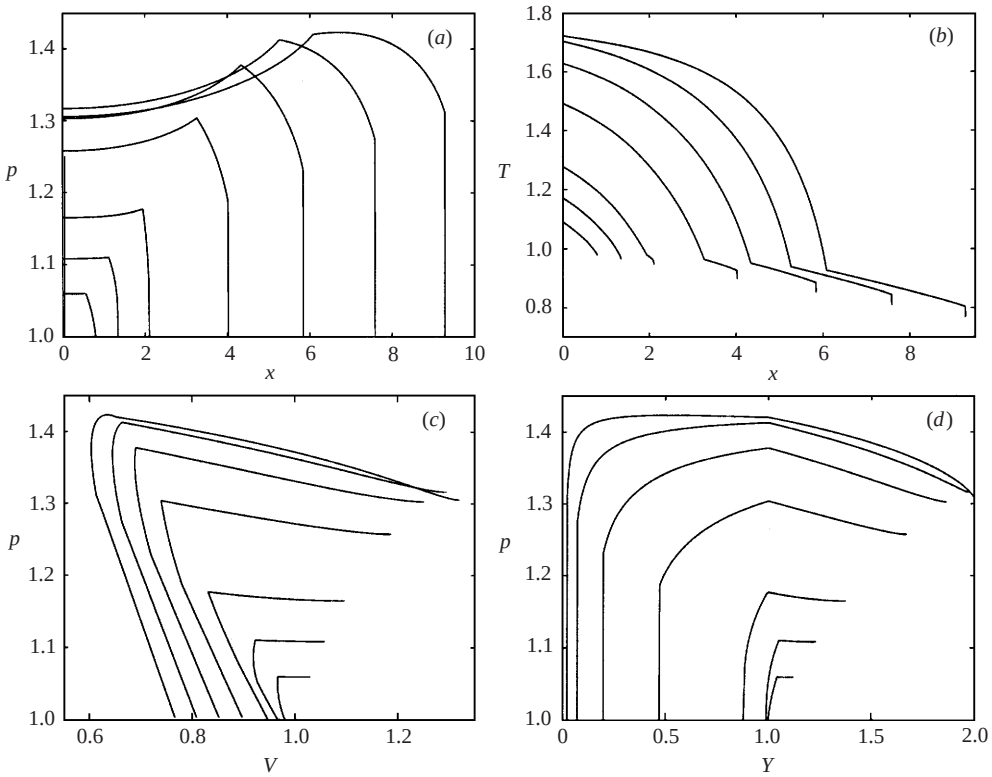

FIGURE 5. (*a*) Pressure profiles, (*b*) temperature profiles, (*c*) p, V diagrams and (*d*) p, Y diagrams for $a = 0.5$ and $k = 0.25$ at times 0.500, 0.980, 1.67, 3.39, 5.02, 6.59 and 8.14.

and further behind the shock. The p, V diagrams show that at this stage the flow consists of a shock followed by an unsteady and expansive induction region, which is in turn followed by the MRZ which is at almost constant pressure, and finally an inert expansion back to the wall. The expansive nature of the IZ and the resulting deceleration of the shock lead to a widening of the IZ behind the shock due to the lower and lower temperatures in this region. The rapid decoupling between the shock and main reaction zone can be clearly seen in the profiles of the temperature. Hence for $a = 0.5$ and $k = 5$, a detonation wave fails to be ignited.

While the failure process seen in figure 4 is somewhat similar to that for $a = 6$ for one-step chemistry in KSQH, the circumstances under which the failure occurs are quite different. In the one-step case, failure only occurs for sufficiently high gradients, and under these circumstances the events leading up to shock formation are highly unsteady (KSQH), whereas in the current situation, there is a still a high degree of quasi-steadiness in the fast-flame part of the MRZ (figure 3). More importantly, unless the gradient is very high (in which case the shock and reaction zone never begin to couple, see the case $k = 0.25$ below) for one-step kinetics, the detonation fails after a *secondary* shock forms. The failure only occurs after this secondary shock has overtaken the leading shock. In the current case for the two-step model, no secondary shock forms and it is the coupling and subsequent decoupling of the leading shock which leads to the failure.

Figure 5 shows the evolution when the MRZ time scale is now long compared to that of the IZ ($k = 0.25$, $a_{\mathrm{MRZ}} = 2.0$). At early times the MRZ consists of an unsteady

compressive region followed by a slightly expansive region which occurs at almost constant pressure. In this case a shock forms while the fuel at $x = 0$ is far from being completely burnt, and it forms at the head of the compressive region of the MRZ, i.e. at the transition point. This rather weak shock subsequently propagates ahead of the transition point into the induction zone and slowly strengthens. The p, V diagrams reveal that at this stage the flow consists of the weak shock, an unsteady compressive induction region behind the shock, followed by the MRZ which now consists entirely of a quasi-steady fast flame (although the fuel at $x = 0$ is still not completely burnt). However, the p, V diagrams also show that the fast flame is not accelerating towards the shock (neither the slopes of the shock or the fast flame are noticeably increasing) and hence in this case there is no further coupling between the shock and MRZ. Indeed, although the shock strength increases it does not do so sufficiently quickly as it propagates to prevent the post-shock temperature decreasing due to the temperature gradient it is propagating through, as can be seen in the temperature profiles. Not only is the post-shock temperature decreasing, the shock is also propagating into decreasing values of ξ, and hence the induction time of sequentially shocked particles increases rapidly. Thus the transition point continually recedes from the shock, as is clearly revealed in the temperature profiles. This complete lack of coupling of the shock and reaction zone is similar to that seen in the one-step case when the gradient is very high. Indeed, the pressure and temperature profiles bear some similarities to those for the case $a = 8$ in KSQH, although the reaction zone is very much thinner in the one-step case (for the latest time shown in figure 5 for the two-step case the MRZ extends from the transition point nearly all the way back to $x = 0$).

5.3. *Case II:* $a = 0.1$

We now consider the case of a shallower temperature gradient of $a = 0.1$. In this case the transition point initially propagates away from $x = 0$ at speed 10 and the spontaneous wave concept predicts that it becomes subsonic only when the transition point has travelled a distance $x = 18.7$ (at $\tau = 6.9$). Now $a < 1/D_{CJ}$ so that the high-k analysis predicts that the whole of the MRZ will be a quasi-steady weak detonation which will transition to a strong detonation as it slows below the CJ speed. The analysis in § 4 predicts that a shock will first form at $x = 12.8$.

Figure 6 shows pressure and temperature profiles and p, V and p, Y diagrams for rapid heat release rate ($k = 100$, $a_{\mathrm{MRZ}} = 0.001$). At very early times for this case, the p, V diagram shows that the MRZ consists of a region of almost constant density followed by a small expansion in which the pressure is almost constant, again in agreement with the analysis in § 3. However, for this gradient the fuel at $x = 0$ becomes fully burnt long before a shock forms. Once this occurs, the MRZ begins to propagate away from $x = 0$ and the p, Y diagrams show that the whole of the MRZ then becomes compressive. This compressive MRZ appears as a straight line in the p, V diagram and is followed by a completely unreactive expansion. Hence now the whole of the MRZ consists of a quasi-steady weak detonation, as predicted by the analysis of § 4. Note that the slope of the straight line in the p, V diagrams decreases with time, so that the weak detonation decelerates as it propagates. The p, Y diagrams show that later a small expansive region begins to appear once more in a small region at the end of the MRZ ($Y = 2$), while the compressive region just ahead of this expansion begins to steepen very quickly, resulting in the formation of a shock, this time much nearer the end of the MRZ. The shock first forms at $x = 12.6$, in excellent agreement with the high-k analysis prediction of 12.8. Subsequent to

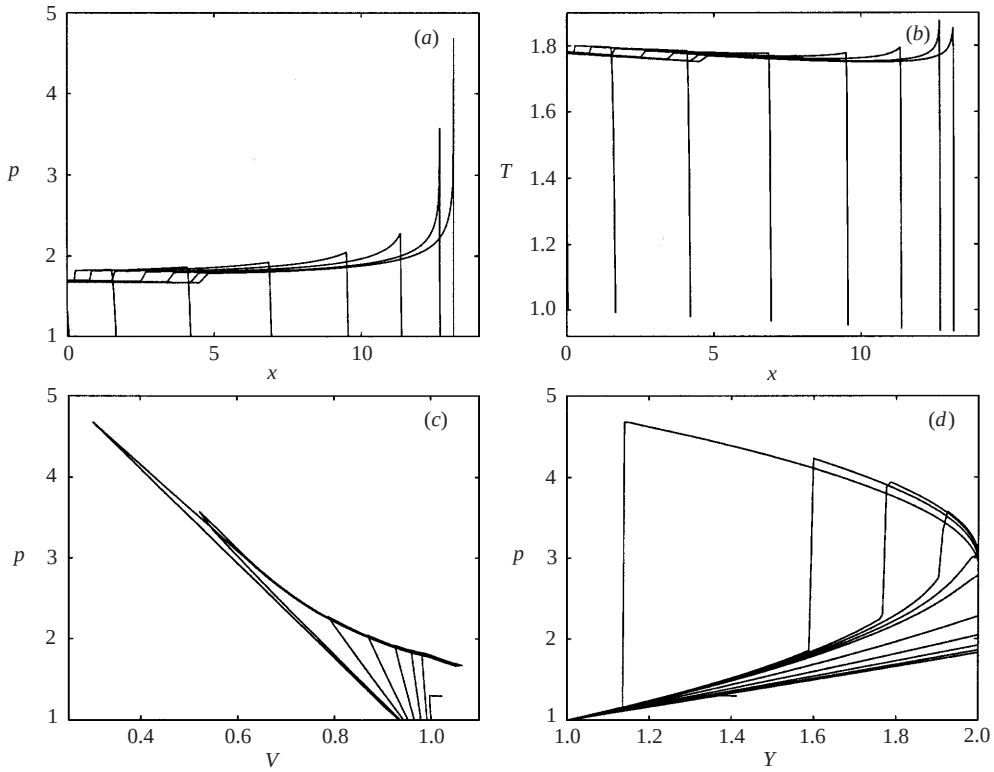

FIGURE 6. (*a*) Pressure profiles, (*b*) temperature profiles, (*c*) p, V diagrams and (*d*) p, Y diagrams for $a = 0.1$ and $k = 100$ at times 0.005, 0.182, 0.536, 1.05, 1.73, 2.34, 2.88 and 3.08 (p, Y diagrams shown at additional times 2.76, 2.82, 2.93 and 2.98 to clarify shock formation).

shock formation, the MRZ consists of the remaining part of the quasi-steady weak detonation followed by the shock, followed in turn by a reactive expansive region which becomes a quasi-steady fast flame.

The above behaviour is very similar to that for $a = 0.1$ in the one-step case studied by KSQH, including the strong forward moving rarefaction which can be seen to form near $x = 0$ in the pressure and temperature profiles, described in KSQH.

The subsequent behaviour, once the shock overtakes the transition (ignition) point, is then very similar to that described above for $a = 0.5$ and $k = 100$, with both the shock and fast flame behind it accelerating until they become fully coupled and a quasi-steady detonation with a widening induction is formed.

Figure 7 shows the evolution for a moderate heat release rate ($k = 5$, $a_{\mathrm{MRZ}} = 0.02$). At early times the behaviour is qualitatively similar to the $k = 100$ case described above. However, while the whole MRZ becomes compressive once the fuel at $x = 0$ becomes completely burnt as above, it does not lie along an entirely straight line in the p, V diagrams and hence it is no longer completely quasi-steady. Again, the region near the end of the MRZ eventually becomes expansive, but the compressive region ahead steepens much less slowly than for $k = 100$. During this stage the transition between the compressive and expansive parts of the MRZ is no longer sharp, indeed the p, V diagrams become highly curved near the maximum pressure point, representing a very unsteady transition zone. The front of the steepening part of the compressive region of the MRZ eventually forms a shock, but now much

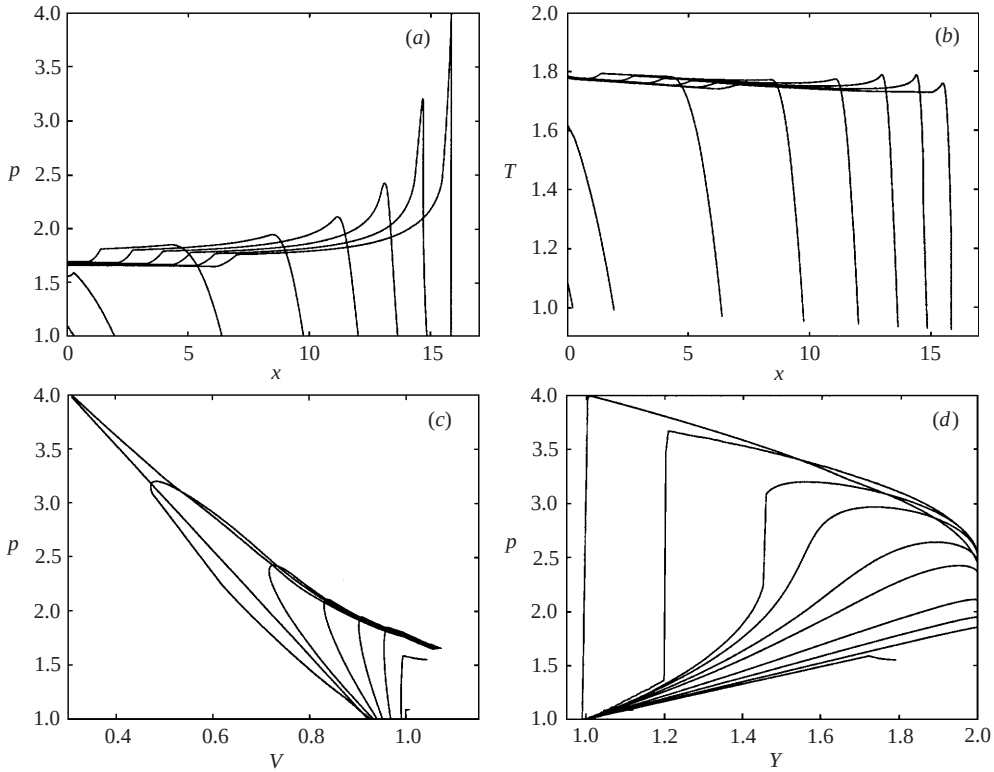

FIGURE 7. (*a*) Pressure profiles, (*b*) temperature profiles, (*c*) p, V diagrams and (*d*) p, Y diagrams for $a = 0.1$ and $k = 5.0$ at times 0.025, 0.217, 0.938, 1.79, 2.59, 3.33, 3.98, 4.54 (p, Y diagrams shown at additional times 3.60, 3.85 and 4.21 to clarify shock formation).

further from the end of the reaction zone, at about $Y = 1.5$. The MRZ subsequently consists of part of a weak detonation, followed by the shock, followed in turn by a highly unsteady transition region and finally a part of a quasi-steady fast flame. As the shock begins to overtake the transition point, the unsteady region disappears and the transition from shock to fast flame becomes sharp.

For this temperature gradient, the detonation does not fail for $k = 5$. Once the shock propagates ahead of the transition point, a quasi-steady detonation is eventually formed, again in a manner very similar to that described above for $a = 0.5$ and $k = 100$, except it takes a much longer time for the shock and fast flame to accelerate and finally completely couple (the shock and MRZ only begin to lie along a common straight line in the (p, V)-plane at about $\tau = 10$ in the current case).

The above evolution for $k = 5$, $a = 0.1$ for the two-step case bears some resemblances to that of $a = 1$ for one-step kinetics in KSQH, including the curved nature of the p, V diagrams before shock formation. The p, Y diagrams differ due to the fact that the MRZ never becomes entirely compressive in the latter case. The shock forms further from the end of the reaction zone for the two-step case than for $a = 1$ in the one-step case. Finally, the strong rarefaction that again forms near $x = 0$ for $k = 5$, which can be seen in the pressure and temperature profiles, is not present in the case $a = 1$ in KSQH.

Figure 8 shows the evolution when the heat release of the MRZ is slow ($k = 0.25$, $a_{\mathrm{MRZ}} = 0.4$). It can be seen that even for the shallower gradient of $a = 0.1$, the

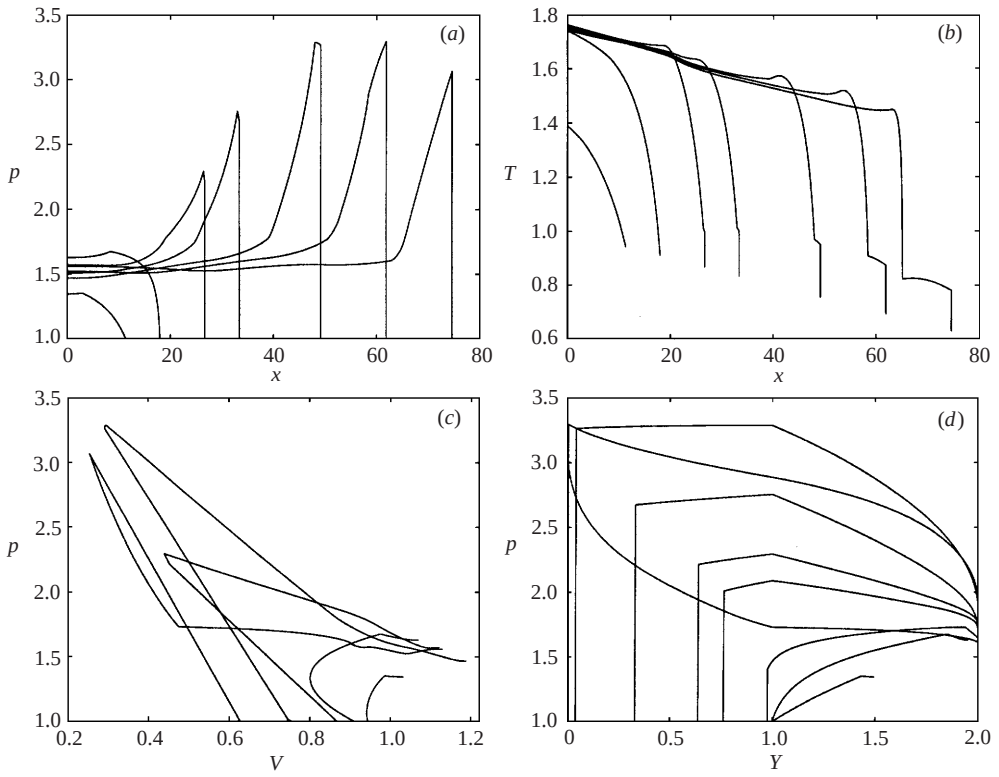

FIGURE 8. (*a*) Pressure profiles, (*b*) temperature profiles, (*c*) p, V diagrams and (*d*) p, Y diagrams for $a = 0.1$ and $k = 0.25$ at times 2.31, 6.22, 12.9, 17.2, 26.8, 34.5 and 42.8 (p, Y diagrams shown at additional times 7.99 and 15.2 to clarify shock formation and pV diagrams only shown at times 2.31, 6.22, 12.9, 26.8 and 42.8 for clarity).

detonation still fails for $k = 0.25$. Before shock formation, the p, V diagrams can be seen to be very, highly curved and hence the early evolution is very unsteady. At this stage the leading part of the MRZ consists of a compressive region in which pressure and density increase. However the density reaches a maximum (V a minimum) while the pressure continues to increase through the wave. Hence the compressive region is followed by a region where density decreases but pressure increases. In this region the density is everywhere almost equal to its initial value, so particles here are undergoing a constant-volume explosion at the local initial density (cf. § 3). Note that the slopes of the p, V diagrams are positive in this second region, and hence this cannot represent any quasi-steady wave (the slope of such waves plotted in the (p, V)-plane is equal to minus the square of the mass flux through the wave and hence must be negative). This locally constant-volume explosion region is hence entirely unsteady and not wave-like, and it can be seen from the early time p, Y diagrams that the largest part of the MRZ consists of it. When they occur, such unsteady increasing pressure/decreasing density regions occupy only a small part of the reaction zone and the p, V diagrams in the one-step case (e.g. see the case for $a = 4$ in KSQH), while in the current case this region is very pronounced. Finally, there is an expansive part of the MRZ near $x = 0$ which occurs at almost constant pressure.

The shock forms at about the time the fuel at $x = 0$ becomes fully burnt; again it forms at the transition point $Y = 1$. Subsequently a compressive part of the IZ

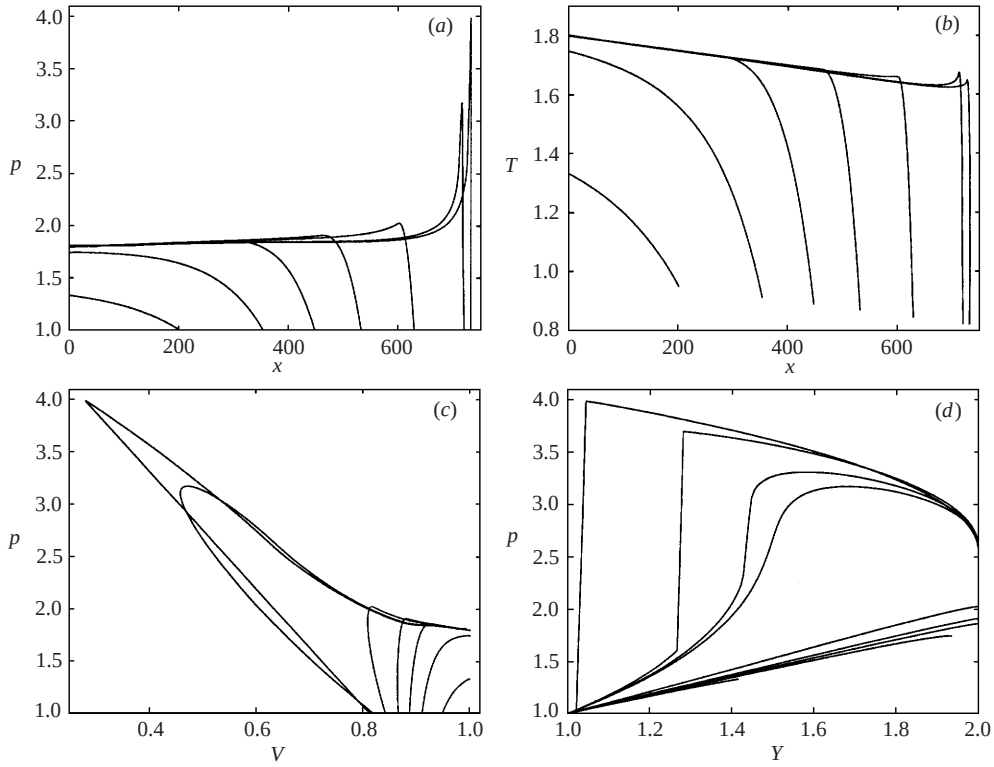

FIGURE 9. (*a*) Pressure profiles, (*b*) temperature profiles, (*c*) p, V diagrams and (*d*) p, Y diagrams for $a = 0.005$ and $k = 0.25$ at times 1.89, 5.96, 11.5, 20.6, 40.8, 80.0 and 87.6 (p, Y diagrams shown at additional times 81.1 and 83.8 to clarify shock formation).

forms behind the shock, and the MRZ becomes a quasi-steady fast flame. The shock and fast flame accelerate but there is no further significant coupling and the shock strength increases too slowly to prevent the shock temperature decreasing. Hence once again the transition point subsequently recedes from the shock, the IZ behind the shock becomes expansive and the shock and MRZ decouple.

5.4. *Case III*: $a = 0.005$

We now consider an extremely shallow gradient when k is also small. Figure 9 shows the evolution when $k = 0.25$ and $a = 0.005$ ($a_{\mathrm{MRZ}} = 0.02$). The transition point now initially propagates extremely rapidly, at speed $200 \gg \gamma^{-1/2}$. The p, V and p, Y diagrams show that initially the whole of the MRZ (apart from a very small expansive region near $x = 0$) consists of an increasing pressure, decreasing density region. During this stage the density remains essentially at its original value (cf. § 3), so that each particle is undergoing a constant-volume explosion at its initial density. Eventually a compressive (increasing pressure and density) region appears just behind the transition point, and hence the slope of the p, V diagrams becomes negative and the evolution begins to become wave-like here. Note however that the extremely rapid transition point has propagated a very long distance before this occurs ($x \approx 500$), into significantly lower temperatures ($T \approx 0.87$). Subsequently, the rest of the MRZ rapidly becomes compressive, but remains highly unsteady, and then an increasing expansive region of the MRZ forms at its rear. However, now the p, V diagram shows that in this case the expansive part of the MRZ does not lie along an entirely straight

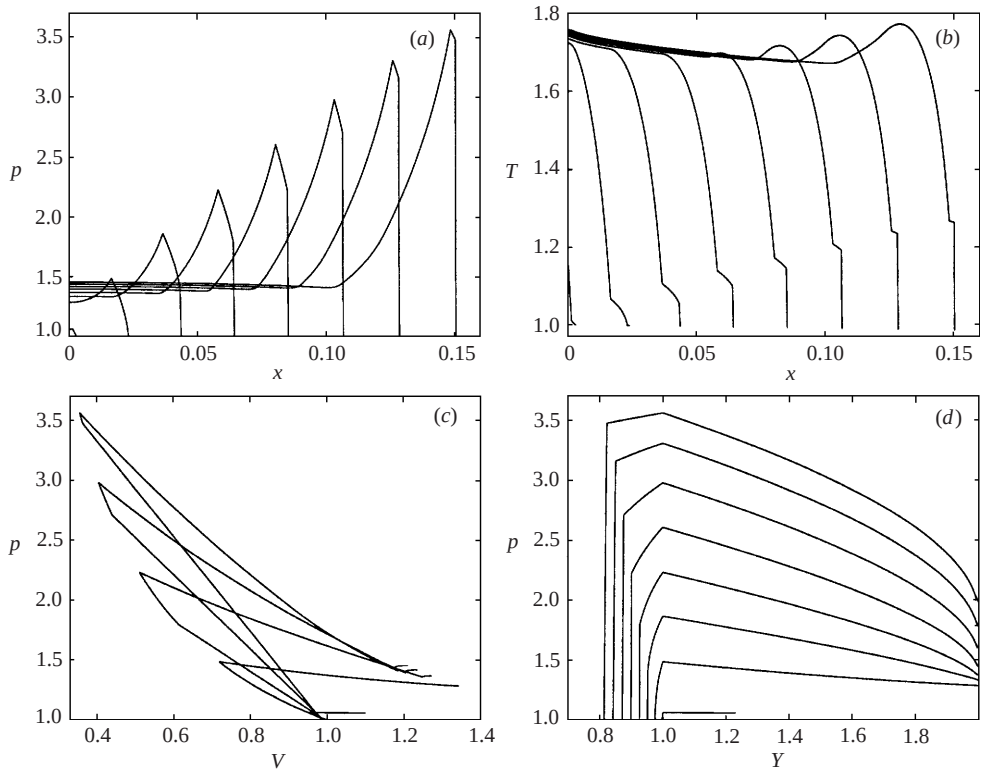

FIGURE 10. (*a*) Pressure profiles, (*b*) temperature profiles, (*c*) p, V diagrams and (*d*) p, Y diagrams for $a = 2$ and $k = 100.0$ at times 0.003, 0.021, 0.038, 0.054, 0.068, 0.081, 0.093 and 0.104 (p, V diagrams only shown at times 0.003, 0.021, 0.054, 0.081 and 0.104 for clarity).

line, so is no longer quasi-steady. The shock forms inside the MRZ at about $Y = 1.4$, which subsequently strengthens as it propagates through the remainer of the MRZ, until it overtakes the transition point, but the fast flame behind the shock remains unsteady in this case. Even for this extremely shallow gradient the detonation still eventually fails when $k = 0.25$.

5.5. *Case IV:* $a = 2$

Finally, we consider a case where the transition point propagates subsonically from the outset when the heat release is rapid. Figure 10 shows the early time evolution when $a = 2$ with $k = 100$ ($a_{\mathrm{MRZ}} = 0.02$). In this case the ignition point initially propagates at speed $0.5 < \gamma^{-1/2}$ so that the disturbance from the MRZ will immediately propagate ahead of the ignition point into the MRZ, and alter the ignition path from that predicted by the spontaneous wave concept given by (2.18). Figure 10 shows that in this case even at very early times the MRZ consists entirely of a quasi-steady fast flame (initially at almost constant pressure throughout), while there is an unsteady and compressive disturbed part of the IZ ahead of the ignition point. This disturbed part of the IZ begins to steepen at its front and eventually a shock forms there. Hence at this stage the flow consists of a shock followed by the compressive part of the IZ, followed in turn by the quasi-steady fast flame MRZ. The shock subsequently strengthens rapidly and both shock and fast flame accelerate, while the IZ behind the shock becomes less and less compressive. The evolution in this case does not bear much similarity to any case studied in KSQH for one-step kinetics.

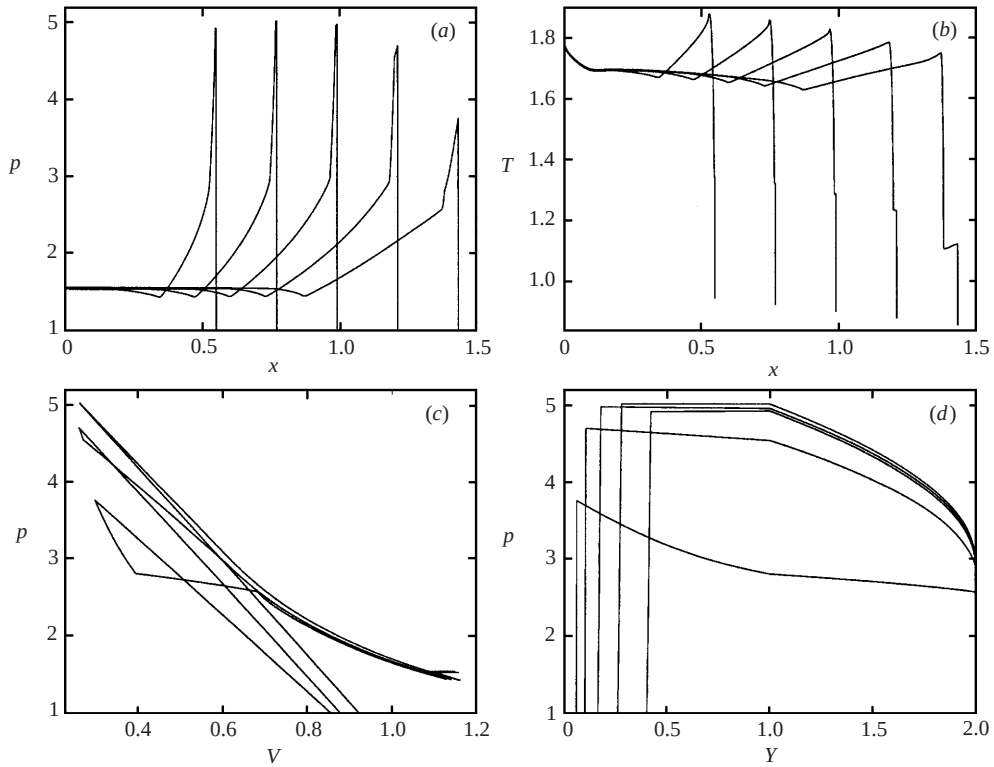

FIGURE 11. (*a*) Pressure profiles, (*b*) temperature profiles, (*c*) p, V diagrams and (*d*) p, Y diagrams for $a = 2$ and $k = 100.0$ at times 0.285, 0.382, 0.480, 0.580 and 0.688 (p, V diagrams only shown at times 0.382, 0.580 and 0.688 for clarity).

Figure 11 shows the later time evolution. Initially the shock and fast flame continue to accelerate but before they couple completely the post-shock temperature begins to decrease and once again the detonation fails, with the IZ becoming expansive and the ignition point rapidly receding from the shock. Note that again no secondary shock is formed before the failure, even when the rate of heat release is quite rapid ($k = 100$).

6. Conclusions

The purpose of this paper has been to investigate the ignition of a detonation from a linear temperature gradient for a two-step kinetics model which mimics the main features of chain-branching chemistry, and to compare and contrast the results with those of previous work which employed simple one-step chemistry.

In our model the induction zone (IZ) stage is assumed to be thermally neutral since most chain-initiation steps are only very slightly endothermic. This has a profound effect on the validity of Zeldovich's spontaneous wave concept, which ignores gasdynamics. For a single exothermic reaction, the heat release in the induction stage switches on gasdynamics and produces a balance between linearized acoustics and the temperature-sensitive heat release rate (KSQH). The result is that even when the thermal runaway point propagates supersonically, it does so through an evolving induction region and hence the spontaneous wave concept becomes invalid: the thermal runaway path may be quite different to the spontaneous wave path.

In the two-step model however, if the temperature gradient is sufficiently shallow ($a < \gamma^{-1/2}$) so that the transition point marking the end of the IZ initially propagates supersonically, then there is no gasdynamic evolution in the IZ and hence the transition point follows the spontaneous wave path, which can be determined using only the initial conditions.

This result in fact makes analysis of the two-step model much easier than for one-step kinetics when $a < \gamma^{-1/2}$ and the transition point propagates supersonically. The initial stages of the evolution of the main reaction zone (MRZ) located behind the transition point is then amenable to a high-activation-temperature asymptotic analysis which has a simple solution. The analysis is valid for $\tau = O(1)$ when the MRZ time scale is long compared to that of the IZ ($k \ll 1$) or for very early time ($\tau \ll 1$) when the MRZ time is comparable with or shorter than the IZ scale. This analysis reveals that initially there is a balance between linearized acoustics and heat release in the MRZ. It also shows that the MRZ is separated at a discontinuity in the gradients of the gasdynamical variable into two distinct regions by the sound wave which leaves $x = 0$ at $\tau = 0$ (where heat release first begins). The region between the transition point and the sound wave is compressive, whereas the region between $x = 0$ and the sound wave is expansive. For sufficiently shallow gradients ($a \ll 1$) the density is almost constant at any point within the 'compressive' region, so that each particle undergoes a constant-volume explosion at the local value of the density. Secondly, for large k (rapid heat release) a very simple quasi-steady analysis is possible. For $a < 1/D_{CJ}$ this analysis predicts the location of shock formation.

Numerical simulations were then used in order to investigate the evolution. For shallow gradients such that the transition point propagates supersonically, the path and speed of the transition point are determined only by the temperature gradient as measured in the IZ length scale, a, independent of the ratio of IZ to MRZ scales, k. However, for fixed a the evolution of the MRZ and whether or not a detonation is successfully ignited depends critically on k. If $k \gg 1$ (short MRZ) then successful ignition is guaranteed if $a < 1/D_{CJ}$. On the other hand if the MRZ length is comparable with or longer than that of the IZ, the evolution may be quite different and the outcome less certain, for example involving highly unsteady processes. For a detonation to be ignited, the numerics show that the temperature gradient must be sufficiently shallow on the MRZ length scale, $a_{\mathrm{MRZ}} = a/k$, which requires $a \ll 1$. Indeed, for a detonation wave to be ignited for a given temperature gradient, a, the heat release rate must be sufficiently high that the shock strength is increased rapidly enough to prevent the shock temperature decreasing. As a consequence, for a detonation to form when k is moderate or small, the transition point must initially propagate supersonically and continue to do so for a time comparable to $1/k$. Another result is that successful ignition in these cases does not involve the formation of a secondary shock, unlike some cases for the one-step kinetics (KSQH).

The conclusion is that the evolution to detonation from temperature non-uniformities may be qualitatively different for one-step kinetics models than for chain-branching kinetic models and that the evolution may be very different in different fuels governed by chain-branching chemistry, such as hydrogen–oxygen, hydrocarbon–oxygen as well as condensed-phase explosives, for the same initial disturbance.

The authors are grateful to Mantis Numerics Ltd. for providing μCobra. G. J. S. would like to thank the Department of Theoretical and Applied Mechanics at UIUC, where this work began, for its hospitality. The work was supported by the Air Force Office of Scientific Research.

REFERENCES

Bdzil, J. B. & Kapila, A. K. 1992 Shock-to-detonation transition: A model problem. *Phys. Fluids* A **4**, 409–418.

Clarke, J. F., Kassoy, D. R., Meharzi, N. E., Riley, N. & Vasantha, R. 1990 On the evolution of plane detonations. *Proc. R. Soc. Lond.* A **429**, 259–283.

Clarke, J. F. & Nikiforakis, N. 1999 Remarks on diffusionless combustion. *Phil. Trans. R. Soc. Lond.* A **357**, 3605–3620.

Clifford, L. J., Milne, A. M., Turanyi, T. & Boulton, D. 1998 An induction parameter model for shock-induced hydrogen combustion simulations. *Combust. Flame* **113**, 106–118.

Dold, J. W. & Kapila, A. K. 1991 Comparison between shock initiations of detonation using thermally-sensitive and chain-branching chemical models. *Combust. Flame* **85**, 185–194.

Dold, J. W., Kapila, A. K. & Short, M. 1991 Theoretical description of direct initiation of detonation for one-step chemistry. In *Dynamic Structure of Detonation In Gaseous and Dispersed Media* (ed. A. A. Borissov), pp 109–141. Kluwer.

Dold, J. W., Short, M., Clarke, J. F. & Nikiforakis, N. 1995 Accumulating sequence of ignitions from a propagating pulse. *Combust. Flame* **100**, 465–473.

Dremin, A. N. 1999 *Toward Detonation Theory*. Springer.

Fickett, W. & Davis, W. C. 1979 *Detonation*. University of California Press.

Fickett, W., Jacobson, J. D. & Schott, G. L. 1972 Calculations of pulsating one-dimensional detonations with induction-zone kinetics. *AIAA J.* **10**, 514–516.

Guirguis, R., Oran, E. S. & Kailasanath, K. 1986 The effect of energy release on the regularity of detonation cells in liquid nitromethane. In *Twenty-first Symp. (Intl) on Combustion*, pp. 1639–1668. Pittsburgh: the Combustion Institute.

He, L. & Clavin, P. 1992 Critical conditions for detonation initiation in cold gaseous mixtures by nonuniform hot pockets of reactive gas. In *Twenty-fourth Symp. (Intl) on Combustion*, pp. 1861–1867. Pittsburgh: the Combustion Institute.

Jackson, T. L., Kapila, A. K. & Stewart, D. S. 1989 Evolution of a reaction center in an explosive material. *SIAM J. Appl. Maths* **49**, 432–458.

Kapila, A. K., Schwendeman, D. W., Quirk, J. J. & Hawa, T. 2002 Mechanisms of detonation formation due to a temperature gradient. *Combust. Theory. Model* **6**, 553–594 (referred to herein as KSQH).

Khokhlov, A. M., Oran, E. S. & Wheeler, J. C. 1997 A theory of deflagration-to-detonation transition in unconfined flames. *Combust. Flame* **108**, 503–517.

Makhviladze, G. M. & Rogatykh, D. I. 1991 Nonuniformities in initial temperature and concentration as a cause of explosive chemical reactions in combustible gases. *Combust. Flame* **87**, 347–356.

Nikiforakis, N. & Clarke, J. F. 1996 Quasi-steady structures in the two-dimensional initiation of detonations. *Proc. R. Soc. Lond.* A **452**, 2023–2042.

Sharpe, G. J. 2002 Shock-induced ignition for a two-step chain-branching kinetics model. *Phys. Fluids* **14** (to appear).

Sharpe, G. J. & Falle, S. A. E. G. 2000 One-dimensional nonlinear stability of pathological detonations. *J. Fluid Mech.* **414**, 339–366.

Short, M. 1997 On the critical conditions for the initiation of a detonation in a nonuniformly perturbed reactive fluid. *SIAM J. Appl. Maths* **57**, 1242–1280.

Short, M. 2001 A nonlinear evolution equation for pulsating Chapman–Jouguet detonations with chain-branching kinetics. *J. Fluid Mech.* **430**, 381–400.

Short, M. & Quirk, J. J. 1997 On the nonlinear stability and detonability limit of a detonation wave for a model three-step chain-branching reaction. *J. Fluid Mech.* **339**, 89–119.

Short, M. & Sharpe, G. J. 2002 Numerical simulations of pulsating detonations with chain-branching kinetics. *Combust. Theory Model*, submitted.

Singh, G. & Clarke, J. F. 1992 Transient phenomena in the initiation of a mechanically driven plane detonation. *Proc. R. Soc. Lond.* A **438**, 23–46.

Taki, S. & Fujiwara, T. 1978 Numerical analysis of two-dimensional nonsteady detonation. *AIAA J.* **16**, 73–77.

Zeldovich, Y. B. 1980 Regime classification of an exothermic reaction with nonuniform initial conditions. *Combust. Flame* **39**, 211–214.